EVALUATION OF RADIATION INDUCED BYSTANDER EFFECT (RIBE) INVOLVING MCF-7 AND HFOB 1.19 CELLS FOLLOWING BISMUTH OXIDES NANOPARTICLES TREATMENT IN RADIOTHERAPY

NUR HAMIZAH BINTI MOHD ZAINUDIN

UNIVERSITI SAINS MALAYSIA

2021

EVALUATION OF RADIATION INDUCED BYSTANDER EFFECT (RIBE) INVOLVING MCF-7 AND HFOB 1.19 CELLS FOLLOWING BISMUTH OXIDES NANOPARTICLES TREATMENT IN RADIOTHERAPY

by

NUR HAMIZAH BINTI MOHD ZAINUDIN

Thesis submitted in fulfilment of the requirements

for the degree of

Doctor of Philosophy

SEPTEMBER 2021

ACKNOWLEDGEMENT

In the name of Allah SWT the Most Gracious and the Most Merciful. Praises be to Allah for His endless blessings for the completion of this thesis. My warmest appreciation goes to my kind supervisor, Dr Wan Nordiana Wan Abd Rahman for her continuous guidance and motivation throughout my PhD journey. Special thanks to my co-supervisor Professor Dr. Khairunisak Abdul Razak for her support and assistance during my candidature. Deepest acknowledgment to Mdm. Norhayati Dollah, Mr Reduan Abdullah and all staffs of the Department of Nuclear Medicine, Radiotherapy and Oncology at the Hospital Universiti Sains Malaysia for their time and persistent help during my data collection process. Special thanks to Universiti Science Malaysia for the Research University Grant (RUI.1001/PPSK/8012212). My special gratitude goes to Malaysia Ministry of Higher Education for Skim Latihan Akademik Bumiputra (SLAB) scholarship and also to Universiti Sultan Zainal Abidin for financial support and study leaves for my PhD study.

I am eternally grateful to my beloved family especially my beloved parent, Che Meriam Mat Harun and Zakaria Mohd Nor, my parent in-law, Anwa Sulaiman and Nooresah Miskam and also my siblings for their d'ua and encouragement during the challenging time of my doctorate study. My deepest appreciation belongs to my greatest supporter, my husband Mohd Hassani Anwa and my beautiful daughter Putri Nur Iman for their endless love, d'ua, sacrifice, patience, understanding and always be there for me all this while through thick and thin. This work is specially dedicated to my beloved family and my late father Mohd Zainudin Saat. Special appreciation to my postgraduates colleagues; Jo, Belle, Nashrul, Afiq, Emi, Fazi and Amirah for their assistance and support throughout this unforgettable journey.

TABLE OF CONTENT

ACKNOWLEDGEMENT ii

TABLE OF CONTENT iii

LIST OF TABLES ix

LIST OF FIGURES x

LIST OF ACRONYMS, ABBREVIATIONS AND SYMBOLS xvii

ABSTRAK xxi

ABSTRACT xxiii

CHAPTER 1 INTRODUCTION 1

1.1 Research Background 1

1.2 Problem Statement 4

1.3 Research Scope 6

1.4 Objective of the Study 7

1.5 Thesis Outline 7

CHAPTER 2 LITERATURE REVIEW 9

2.1 Radiotherapy and Challenges 9

2.2 Radiation Biology 10

2.2.1 Radiobiology and Radiation Injury Mechanism 10

2.2.2 Non-Targeted Effect of Radiation 18

2.3 Radiation-Induced Bystander Effect 21

2.4 Cell Signaling, Communication and Bystander Effect Pathways 24

2.5 Types of Bystander Effect in Non-irradiated Cells 27

2.6 Mechanisms in Radiation-Induced Bystander Non-Targeted Effects 29

2.7 Factors Related to RIBE 34

2.7.1 Radiation dose response on RIBE 34

2.7.2 Cell Types Response in RIBE 36
2.7.3 Effect of Beam Quality on Bystander Effects 39
2.8 Nanomedicine 41
2.8.1 Introduction to Nanomedicine 41
2.8.2 Nanoparticles as Radiosensitizer 43
2.8.3 Biological Response and Challenges due to Nanoparticles 47
2.8.4 Effect of nanoparticles on targeted and non-targeted cells 49
CHAPTER 3 MATERIALS AND METHODS 51
3.1 Flowchart of Research Methodology 52
3.2 Bismuth Oxide Nanoparticles (Bi_2O_3 NPs) 54
3.2.1 Synthesis and Characterization of Bi_2O_3 NPs 54
3.2.2 Preparation of Bi_2O_3 NPs 55
3.3 Cell lines and Cell Culture Procedures 56
3.4 Cytotoxicity Assay 57
3.5 Cellular Uptake of Bi_2O_3 Nanoparticles 58
3.5.1 Flow Cytometry Analysis 58
3.5.2 Bright Field Microscopic Analysis 60
3.6 Irradiation Setup 60
3.6.1 Cell Sample Preparation 60
3.6.2 Photon Beam Radiotherapy 61
3.6.3 Electron Beam Radiotherapy 62
3.6.4 High Dose Rate Brachytherapy 63
3.7 Collection of Irradiated-Cell Conditioned Medium (ICCM) 64
3.8 PrestoBlue Cell Viability Assay 65
3.9 Colony Forming Assay 67

3.10 Measurement of Intracellular Reactive Oxygen Species (ROS) 68
3.11 Fourier Transform Infrared (FTIR) Spectroscopy 69
3.11.1 Preparation of Cell Samples 69
3.11.2 ATR – FTIR Spectroscopic measurement 70
3.11.3 Spectral Data Preprocessing 71
3.12 Apoptosis Assay 72
3.13 Statistical Analysis 73
3.14 Dose Verification 74
3.14.1 Preparation of Film Samples 74
3.14.2 Film Scanning and Analysis 75
CHAPTER 4 RESULTS AND DISCUSSION 77
4.1 Cytotoxicity Analysis 78
4.1.1 Cytotoxicity of Bi_2O_3 NPs on MCF-7 and hFOB 1.19 cells 78
4.1.2 Comparison of Cytotoxicity Analysis on MCF-7 and hFOB 1.19 cells 80
4.1.3 Discussion 82
4.2 Cellular Uptake Analysis 86
4.2.1 Flow Cytometry Analysis 86
4.2.2 Bright Field Microscopic Analysis 88
4.2.3 Discussion 89
4.3 RIBE Analysis in Bystander Cells 93
4.3.1 Short term and Long term effect of RIBE 94
4.3.1 (a) Cell Viability Analysis in MCF-7 and hFOB 1.19 cells 94
4.3.1 (a)(i) Photon Beam Radiotherapy 94

4.3.1 (a)(ii) Electron Beam Radiotherapy 96
4.3.1 (a)(iii) High Dose Rate Brachytherapy 98
4.3.1 (b) Cell Survival Analysis 99
4.3.1 (b)(i) Photon Beam Radiotherapy 100
4.3.1 (b)(ii) Electron Beam Radiotherapy 102
4.3.1 (b)(iii) High Dose Rate Brachytherapy 104
4.3.1 (c) Discussion 105
4.3.1 (c)(i) Short-term and long-term effect of RIBE 105
4.3.1 (c)(ii) Cell Types Effect on RIBE 109
4.3.1 (c)(iii) Effect of Radiation Dose on RIBE 114
4.3.2 Reactive Oxygen Species (ROS) in Bystander Cells 117
4.3.2 (a) Photon Beam Radiotherapy 117
4.3.2 (b) Electron Beam Radiotherapy 119
4.3.2 (c) High Dose Rate Brachytherapy 121
4.3.2 (d) Discussion 122
4.4 Effect of Bi_2O_3 NPs application on RIBE 126
4.4.1 Effect of Bi_2O_3 NPs on Viability of Bystander Cells 126
4.4.1 (a) Photon Beam Radiotherapy 126
4.4.1 (b) Electron Beam Radiotherapy 129
4.4.1 (c) High Dose Rate Brachytherapy 130
4.4.2 Effect of Bi_2O_3 NPs on Survival of Bystander Cells 132
4.4.2 (a) Photon Beam Radiotherapy 132
4.4.2 (b) Electron Beam Radiotherapy 134
4.4.2 (c) High Dose Rate Brachytherapy 136

4.4.3 ROS Generation in Bystander Cells with Bi_2O_3 NPs Application ... 138
4.4.3 (a) Photon Beam Radiotherapy ... 138
4.4.3 (b) Electron Beam Radiotherapy ... 139
4.4.3 (c) High Dose Rate Brachytherapy ... 141
4.4.4 Discussion ... 142
4.5 DNA Damage Evaluation in the Bystander Cells ... 146
4.5.1 Fourier Transform Infrared (FTIR) Spectroscopy Analysis ... 146
4.5.2 Discussion ... 153
4.6 Apoptosis pathway in response to RIBE ... 158
4.6.1 Apoptosis Analysis ... 158
4.6.2 Discussion ... 163
4.7 Influence of Different Irradiation Parameters on RIBE ... 167
4.7.1 Effect of Radiation Types and Energy ... 167
4.7.1 (a) Cell Viability in Bystander Cells ... 167
4.7.1 (b) Cell Survival Analysis in Bystander Cells ... 170
4.7.1 (c) ROS generation in Bystander Cells ... 174
4.7.2 Discussion ... 178
4.8 Radiation Dose Verification ... 181
4.8.1 Photon Beam Radiotherapy ... 181
4.8.2 Electron Beam Radiotherapy ... 184
4.8.3 High Dose Rate Brachytherapy ... 187
CHAPTER 5 CONCLUSION ... 189
5.1 Conclusion ... 189
5.2 Limitation and Future Directions ... 190
REFERENCES ... 192

APPENDICES

APPENDIX A PREPARATION OF MAIN STOCK DILUTION OF Bi_2O_3NPs

APPENDIX B CELL VIABILITY OF MCF-7 AND hFOB 1.19 CELLS

APPENDIX C DOSE VERIFICATION

APPENDIX D PUBLICATION LISTS

APPENDIX E CONFERENCE PRESENTATIONS

LIST OF TABLES

Page

Table 4.1 Estimated dose received by the targeted cells during 6 MV photon beam. 182

Table 4.2 Estimated dose received by the targeted cells during 10 MV photon beam. 183

Table 4.3 Estimated dose received by the targeted cells during 6 MeV electron beam..... 185

Table 4.4 Estimated dose received by the targeted cells during 12 MeV electron beam..... 186

Table 4.5 Estimated dose received by the targeted cells during HDR Brachytherapy..... 188

LIST OF FIGURES

Page

Figure 2.1 The time-scale of radiation effects on biological systems (adapted from van der Kogel, 2009)..... 11

Figure 2.2 The possible radiation injury mechanism, direct and indirect actions of radiation (adapted from Desouky et al., 2015). 13

Figure 2.3 Two ways of radiation action (adapted from Baskar et al., 2014). 14

Figure 2.4 The illustration of different radiation-induced cell death mechanisms (adapted from Minafra & Bravatà, 2015). 17

Figure 2.5 A timeline on bystander effects study over the last hundred years. (adapted from Carmel Mothersill, Rusin, Fernandez-Palomo, & Seymour, 2017). 19

Figure 2.6 Schematic representation of radiation-induced signaling effects in non-targeted and targeted cells. Irradiated cells are shown in red; unirradiated cells in blue (adapted from Butterworth et al., 2013). 20

Figure 2.7 A model of radiation-induced bystander effect (RIBE) responses in the cells (adapted from Klammer, Mladenov, Li, & Iliakis, 2015). 23

Figure 2.8 The binding of extracellular signal molecules to either cell-surface receptors or intracellular receptors (adapted from Alberts et al., 2002). 24

Figure 2.9 Schematic representation of bystander effects induced by radiation to the adjacent cells and distanced organs (adapted from Baskar et al., 2014). 26

Figure 2.10 The Lewis dot diagrams of common ROS and RNS. The unpaired electrons are designated in red (adapted from Klammer et al., 2015). 30

Figure 2.11 The illustration of physical mechanism on how metallic nanoparticles enhance radiation sensitivity in cells. (adapted from Paro & Shanmugam, 2017)..... 45

Figure 2.12 The illustration of the biological mechanism involved in nanoparticles radiosensitization (adapted from Sun et al., 2020)..... 47

Figure 3.1 The flowchart of the experiment in this study..... 53

Figure 3.2 (A) The stirring process of $Bi(NO_3)_3.5H_2O$ and 3 mMol/L of Na_2SO_4 which were dissolved in 40 ml of distilled water solution, (B) the solution was continuously stirred after addition of NaOH, and (C) the form yellowish precipitates solution was formed and then subjected for hydrothermal procedure..... 54

Figure 3.3 Bismuth oxide nanoparticles (Bi_2O_3 NPs) was in powder form after air dried at 80°C. 55

Figure 3.4 The cell lines used in this study, (A) human breast cancer cells (MCF-7) and (B) human normal osteoblast cells (hFOB 1.19). Magnification at 40x. 56
Figure 3.5 The illustration of experiment workflow for cytotoxicity assay. 58
Figure 3.6 The illustration of flow cytometry analysis workflow for nanoparticles cellular uptake. 59
Figure 3.7 The experiment setup during photon beam irradiation. 62
Figure 3.8 The experiment setup during electron beam irradiation. 63
Figure 3.9 The experiment setup during HDR brachytherapy. 64
Figure 3.10 Microselectron HDR Brachytherapy. 64
Figure 3.11 The flowchart of the bystander effects experiment for this study. 65
Figure 3.12 The illustration of PrestoBlue cells viability procedure. 66
Figure 3.13 The bystander cells were treated with ICCM for 9 to 14 days for colony-forming assay. 68
Figure 3.14 The illustration of reactive oxygen species (ROS) measurement. 69
Figure 3.15 Bruker Tensor 27 spectrometer. 71
Figure 3.16 The representative photograph of cell suspension pipetted onto the ATR crystal. 71
Figure 3.17 An illustration of the experimental workflow for apoptosis analysis. 73
Figure 3.18 The EBT3 film were placed in the flask for dose verification. 75
Figure 4.1 Cell viability of MCF-7 cells incubated with Bi_2O_3 NPs of different concentration measured at 24, 48 and 72 hours. The values are presented as mean ± SEM. (n=3). $^{**}p < 0.01$ when compared to untreated group. 79
Figure 4.2 Cell viability of hFOB 1.19 cells incubated with Bi_2O_3 NPs of different concentration measured at 24, 48 and 72 hours. The values are presented as mean ± SEM. (n=3). $^{***}p < 0.001$ when compared to untreated group. 80
Figure 4.3 The comparison of cell viability between MCF-7 and hFOB 1.19 after 48 hours incubated with different concentration of Bi_2O_3 NPs. The values are presented as mean ± SEM. (n=3). $^{***}p < 0.001$ when compared to untreated group. $^{*}p < 0.05$ when compared MCF-7 and hFOB 1.19 at 50 µMol/L. 81
Figure 4.4 Scatter analysis of Bi_2O_3 NPs uptake in (A) MCF-7 control cells; (B) MCF-7 cells + 5 µMol/L Bi_2O_3 NPs, (C) hFOB 1.19 control cells; (D) hFOB 1.19 cells + 5 µMol/L Bi_2O_3 NPs cells. Q1 and Q3 quadrants represented a dead cell or cell debris population, whereas the Q2 and Q4 quadrants represented a live cell population. 88

Figure 4.5 Bright field microscopic images of (A) MCF-7 and (B) hFOB 1.19 cells treated with 5 µMol/L of Bi_2O_3 NPs. Magnification at 100x. 89

Figure 4.6 RIBE response between MCF-7 and hFOB 1.19 bystander cells after 48 hours incubation with ICCM from 6 MV photon beam. The values are presented as means ± SEM. (n=3)..... 95

Figure 4.7 RIBE response between MCF-7 and hFOB 1.19 bystander cells after 48 hours incubation with ICCM from 10 MV photon beam. The values are presented as means ± SEM. (n=3)..... 96

Figure 4.8 RIBE response between MCF-7 and hFOB 1.19 bystander cells after 48 hours incubation with ICCM from 6 MeV electron beam. The values are presented as means ± SEM. (n=3). 97

Figure 4.9 RIBE response between MCF-7 and hFOB 1.19 bystander cells after 48 hours incubation with ICCM from 12 MeV electron beam. The values are presented as means ± SEM. (n=3). 98

Figure 4.10 RIBE response between MCF-7 and hFOB 1.19 bystander cells after 48 hours incubation with ICCM from HDR Brachytherapy. The values are presented as means ± SEM. (n=3)..... 99

Figure 4.11 Percentages of survival fraction for MCF-7 and hFOB 1.19 bystander cells after 10 days incubation with ICCM from 6 MV photon beam at different radiation doses. The values are presented as means ± SEM. (n=3). 100

Figure 4.12 Percentages of survival fraction for MCF-7 and hFOB 1.19 bystander cells after 10 days incubation with ICCM from 10 MV photon beam at different radiation doses. The values are presented as means ± SEM. (n=3). 101

Figure 4.13 Percentages of survival fraction for MCF-7 and hFOB 1.19 bystander cells after 10 days incubation with ICCM from 6 MeV electron beam at different radiation doses. The values are presented as means ± SEM. (n=3). 102

Figure 4.14 Percentages of survival fraction for MCF-7 and hFOB 1.19 bystander cells after 10 days incubation with ICCM from 12 MeV electron beam at different radiation doses. The values are presented as means ± SEM. (n=3). 103

Figure 4.15 Percentages of survival fraction for MCF-7 and hFOB 1.19 bystander cells after 10 days incubation with ICCM from HDR Brachytherapy at different radiation doses. The values are presented as means ± SEM. (n=3). 104

Figure 4.16 Relative ROS fluorescence level in MCF-7 and hFOB 1.19 cells receiving ICCM from 6 MV photon beam. The values are presented as means ± SEM. (n=3). 118

Figure 4.17 Relative ROS fluorescence level in MCF-7 and hFOB 1.19 cells receiving ICCM from 10 MV photon beam. The values are presented as means ± SEM. (n=3). 119

Figure 4.18 Relative ROS fluorescence level in MCF-7 and hFOB 1.19 cells receiving ICCM from 6 MeV electron beam. The values are presented as means ± SEM. (n=3). 120

Figure 4.19 Relative ROS fluorescence level in MCF-7 and hFOB 1.19 cells receiving ICCM from 12 MeV electron beam. The values are presented as means ± SEM. (n=3). 121

Figure 4.20 Relative ROS fluorescence level in MCF-7 and hFOB 1.19 cells receiving ICCM from HDR Brachytherapy. The values are presented as means ± SEM. (n=3). 122

Figure 4.21 Cell viability between MCF-7 and hFOB 1.19 bystander cells after 48 hours incubation with ICCM treated with Bi_2O_3 NPs from 6 MV photon beam. The values are presented as means ± SEM. (n=3). 127

Figure 4.22 Cell viability between MCF-7 and hFOB 1.19 bystander cells after 48 hours incubation with ICCM treated with Bi_2O_3 NPs from 10 MV photon beam. The values are presented as means ± SEM. (n=3). 128

Figure 4.23 Cell viability between MCF-7 and hFOB 1.19 bystander cells after 48 hours incubation with ICCM treated with Bi_2O_3 NPs from 6 MeV electron beam. The values are presented as means ± SEM. (n=3). 129

Figure 4.24 Cell viability between MCF-7 and hFOB 1.19 bystander cells after 48 hours incubation with ICCM treated with Bi_2O_3 NPs from 12 MeV electron beam. The values are presented as means ± SEM. (n=3). 130

Figure 4.25 Cell viability between MCF-7 and hFOB 1.19 bystander cells after 48 hours incubation with ICCM treated with Bi_2O_3 NPs from HDR Brachytherapy. The values are presented as means ± SEM. (n=3). 131

Figure 4.26 Survival fraction between MCF-7 and hFOB 1.19 bystander cells after 10 days incubation with ICCM treated with Bi_2O_3 NPs from 6 MV photon beam. The values are presented as means ± SEM. (n=3) 133

Figure 4.27 Survival fraction between MCF-7 and hFOB 1.19 bystander cells after 10 days incubation with ICCM treated with Bi_2O_3 NPs from 10 MV photon beam. The values are presented as means ± SEM. (n=3). $*p < 0.05$ when compared to untreated group. 134

Figure 4.28 Survival fraction between MCF-7 and hFOB 1.19 bystander cells after 10 days incubation with ICCM treated with Bi_2O_3 NPs from 6 MeV electron beam. The values are presented as means ± SEM. (n=3) 135

Figure 4.29 Survival fraction between MCF-7 and hFOB 1.19 bystander cells after incubation with ICCM treated with Bi_2O_3 NPs from

12 MeV electron beam. The values are presented as means ± SEM. (n=3). 136

Figure 4.30 Survival fraction between MCF-7 and hFOB 1.19 bystander cells after 10 days incubation with ICCM treated with Bi_2O_3 NPs from HDR Brachytherapy. The values are presented as means ± SEM. (n=3)..... 137

Figure 4.31 The comparison between relative ROS fluorescence level in MCF-7 and hFOB 1.19 bystander cells receiving treated and untreated ICCM for 6 MV photon beam. The values are presented as means ± SEM. (n=3). 138

Figure 4.32 The comparison between relative ROS fluorescence level in MCF-7 and hFOB 1.19 bystander cells receiving treated and untreated ICCM for 10 MV photon beam. The values are presented as means ± SEM. (n=3). 139

Figure 4.33 The comparison between relative ROS fluorescence level in MCF-7 and hFOB 1.19 bystander cells receiving treated and untreated ICCM for 6 MeV electron beam. The values are presented as means ± SEM. (n=3). 140

Figure 4.34 The comparison between relative ROS fluorescence level in MCF-7 and hFOB 1.19 bystander cells receiving treated and untreated ICCM for 12 MeV electron beam. The values are presented as means ± SEM. (n=3). 141

Figure 4.35 The comparison between relative ROS fluorescence level in MCF-7 and hFOB 1.19 bystander cells receiving treated and untreated ICCM for HDR Brachytherapy. The values are presented as means ± SEM. (n=3). 142

Figure 4.36 The average spectra at 1150 to 950 cm^{-1} for treated and untreated MCF-7 bystander cells incubated with ICCM irradiated with 0, 2 and 12 Gy of 6 MV photon beam, after processing of three individual spectra per sample. 147

Figure 4.37 The second derivative spectra of FTIR spectroscopy for the treated and untreated group of MCF-7 bystander cells incubated with ICCM irradiated with 0, 2 and 12 Gy of 6 MV photon beam, after processing of three individual spectra per sample. 148

Figure 4.38 The average spectra at 1150 to 950 cm^{-1} for the treated and untreated hFOB 1.19 bystander cells incubated with ICCM irradiated with 0, 2 and 12 Gy of 6 MV photon beam, after spectra processing of three individual spectra per sample. 149

Figure 4.39 The second derivative spectra of FTIR spectroscopy for the untreated group of hFOB 1.19 bystander cells incubated with ICCM irradiated with 0, 2 and 12 Gy of 6 MV photon beam, after processing of three individual spectra per sample. 150

Figure 4.40 The changes in the absorbance of the phosphodiester band at 1080 cm^{-1} for treated and untreated (A) MCF-7; and (B) hFOB

1.19 cells in the function of dose. The values are presented as means ± SEM. (n=3)..... 151

Figure 4.41 Change in the absorbance of the phosphodiester band at 1040 cm^{-1} for treated and untreated (A) MCF-7; and (B) hFOB 1.19 cells in function of dose. The values are presented as means ± SEM. (n=3). 152

Figure 4.42 The summary of viable and apoptotic cells percentage (early and late apoptosis) in (A) MCF-7; (B) hFOB 1.19 cells for 6 MV photon beam. The values are presented as means ± SEM. (n=3)..... 159

Figure 4.43 Annexin-Apoptosis Profile on MCF-7 cells. The scatter plot flow cytometry showing the percentages of early and late apoptosis are indicated for one representative experiment..... 161

Figure 4.44 Annexin-Apoptosis Profile on hFOB 1.19 cells. The scatter plot flow cytometry showing the percentages of early and late apoptosis are indicated for one representative experiment..... 162

Figure 4.45 Comparison of the rate of the apoptotic cell (early and late apoptosis) between MCF-7 and hFOB 1.19 cells. The values are presented as means ± SEM. (n=3). 163

Figure 4.46 Comparison of cell viability between radiation types for (A) MCF-7 and (B) hFOB 1.19 bystander cells receiving 0 to 12 Gy ICCM from irradiated cells. The values are presented as means ± SEM. (n=3). 168

Figure 4.47 Comparison of cell viability between radiation types for (A) MCF-7; and (B) hFOB 1.19 bystander cells receiving ICCM treated with Bi_2O_3 NPs at 2, 6 and 12 Gy irradiated cells. The values are presented as means ± SEM. (n=3). 170

Figure 4.48 Comparison of cell survival fraction between radiation types for (A) MCF-7 and (B) hFOB 1.19 bystander cells receiving 0 to 12 Gy ICCM from irradiated cells. The values are presented as means ± SEM. (n=3)..... 171

Figure 4.49 Comparison of cell survival fraction between radiation types for (A) MCF-7 and (B) hFOB 1.19 bystander cells receiving ICCM treated with Bi_2O_3 NPs at 2, 6 and 12 Gy irradiated cells. The values are presented as means ± SEM. (n=3). 173

Figure 4.50 Comparison of ROS level between radiation types for (A) MCF-7 and (B) bystander cells receiving 0 to 12 Gy ICCM from irradiated cells. The values are presented as means ± SEM. (n=3). 175

Figure 4.51 Comparison of ROS level between radiation types for (A) MCF-7 and (B) bystander cells receiving ICCM treated with Bi_2O_3 NPs at 2, 6 and 12 Gy irradiated cells. 177

Figure 4.52 Prescribed dose versus measured dose inside water-filled flask during 6 MV photon beam irradiation. 182

Figure 4.53 Prescribed dose versus measured dose inside water-filled flask during 10 MV photon beam irradiation. 183

Figure 4.54 Prescribed dose versus measured dose inside water-filled flask during 6 MeV electron beam irradiation. 185
Figure 4.55 Prescribed dose versus measured dose inside water-filled flask during 12 MeV electron beam irradiation. 186
Figure 4.56 Prescribed dose versus measured dose inside water-filled flask during HDR Brachytherapy irradiation. 188

LIST OF ACRONYMS, ABBREVIATIONS AND SYMBOLS

$^{\circ}C$	Degree Celsius
^{192}Ir	Iridium-192
$_{137}Cs$	Cesium-137
AuNPs	Gold nanoparticles
AKT	Activated tyrosine kinases
ATR	Attenuated Total Reflectance
Bi_2O_3 NPs	Bismuth oxide nanoparticles
cfCh	Cell-free chromatin
cm	Centimeter
COX-2	Cyclooxygenase-2
CO_2	Carbon dioxide
Dmax	Depth of maximum dose
DMEM	Dulbecco's Modified Eagles Medium
DNA	Deoxyribonucleic acid
DNA-PKcs	DNA-dependent protein kinase catalytic subunit
DSB	Double strand breaks
DSIC	Distant cell signaling intercellular communication
EBRT	External beam radiotherapy
EPR	Enhanced permeability and retention
ERK	Extracellular-regulated kinase
Fe_3O_4 NPs	Iron oxide nanoparticles
FSC	Forward-scattered light
FTIR	Fourier – Transform Infrared

GCSF	Granulocyte colony-stimulating factor
GJIC	Gap junction intercellular communication
Glu-GNP	Glucose-coated gold nanoparticles
Gy	Gray
HDR	High Dose Rate
HO•	Hydroxyl
HR	Homologous recombination
H_2O_2	Hydrogen peroxide
H2AX	Histone protein
ICCM	Irradiated-cell conditioned medium
IL-1β	Interleukin-1β
IL-6	Interleukin-6
IL-8	Interleukin-8
kV	Kilo voltage
keV	Kilo electron volt
LET	linear energy transfer
LINAC	Linear Accelerator
MAPK	Mitogen-activated protein kinase
MeV	Mega electron volt
miRNA	MicroRNAs
ml	Millimeter
mMol/L	Milli mol per liter
mM	Millimolar
MN	Micronuclei
MNPs	Magnetic nanoparticles

MPS	Mononuclear phagocytic system
MU	Monitor unit
MV	Megavoltage
NF-kB	Nuclear factor-κB
NHEJ	Non-homologous end joining
NO	Nitric oxide
O_2^-	Superoxide
ONOO–	Peroxynitrite
OARs	Organs at risk
PBS	Phosphate buffered Saline
PDGF-AA	Platelet-derived growth factor AA
PE	Plating efficiency
piRNA	Piwi-interacting RNA
PTGS2	Prostaglandin-endoperoxide synthase 2
PtNPs	Platinum nanoparticles
RIBE	Radiation-induced bystander effects
RIRE	Radiation-induced rescue effect
RIT	Internal radioisotope therapy
RNA	Ribonucleic acid
RNS	Reactive nitrogen species
RO2•	Alkoxy
ROS	Reactive oxygen species
RT	Radiotherapy
SEM	Scanning electron micrographs
siRNA	Small interfering RNA

SSB	Single strand break
SSC	Side-scattered light
SSD	Source to surface distance
TCP	Tumour control probability
TGF-β	Transforming growth factor-beta
TGF-β1	Transforming growth factor-β1
TiO_2 NPs	Titanium dioxide nanoparticles
TNF-α	Tumour necrosis factor-α
VEGF	Vascular endothelial growth factor
Z	Atomic number
ZnSe	Zinc selenide
α	Alpha
β	Beta
γ	Gamma
µMol/L	Micro Mol per Litre

PENILAIAN KE ATAS *RADIATION INDUCED BYSTANDER EFFECT* (RIBE) MELIBATKAN SEL MCF-7 DAN HFOB 1.19 SETELAH RAWATAN NANOPARTIKEL BISMUTH OKSIDA DALAM RADIOTERAPI

ABSTRAK

Dalam rawatan radioterapi, kajian mendalam telah dijalankan terhadap penggunaan nanopartikel sebagai pemeka sinaran yang berpotensi untuk meningkatkan kesan radiasi terhadap sel kanser. Penggunaan nanopartikel secara berfokus terhadap sel kanser mampu untuk mengurangkan kesan sampingan radiasi terhadap tisu yang sihat. Walau bagaimanapun, penggunaan pemeka sinaran semasa rawatan mungkin menimbulkan kesan sampingan terhadap sel yang tidak disasarkan semasa rawatan iaitu kesan 'bystander'. Kajian ini bertujuan untuk menilai kesan 'bystander' disebabkan penggunaan nanopartikel bismuth oksida (Bi_2O_3 NPs) semasa rawatan radioterapi bagi sel kanser payudara MCF-7 dan juga sel osteoblast hFOB 1.19. Kajian ini menggunakan beberapa jenis sumber radiasi termasuklah sinar foton, sinar elektron dan brakiterapi kadar dos tinggi. Stimulasi kesan 'bystander' dilakukan melalui teknik pemindahan medium. Kebolehhidupan sel, kadar kemandirian sel, spesis oksigen reaktif (ROS), analisis apoptosis dan analisis spektroskopi Fourier Transform Infrared (FTIR) digunakan untuk menilai kesan bystander. Kajian ini menunjukkan bahawa sel 'bystander' MCF-7 dan hFOB 1.19 dapat mengekalkan kebolehhidupan lebih daripada 80% selepas inkubasi selama 48 jam dengan medium terkondisi sel penyinaran (ICCM) yang dirawat dengan Bi_2O_3 NPs. Sel ini juga menunjukkan tindak balas positif untuk mengekalkan kemandirian sel mereka hingga 80% setelah menjalani rawatan dengan ICCM selama 10 hari.

Tahap ROS bagi sel ‘bystander’ meningkat, tetapi penggunaan Bi_2O_3 NPs tidak meningkatkan tahap ROS dengan ketara. Tiada peningkatan yang signifikan terhadap apoptosis bagi sel MCF-7 dan hFOB 1.19 disebabkan oleh dos radiasi atau kesan pengunaan Bi_2O_3 NPs berbanding sel kawalan. Tahap serapan pada gelombang 1080 cm^{-1} (peregangan simetri PO_2^- DNA) setanding dengan kumpulan yang dirawat dan tidak dirawat untuk kedua-dua sel. Amplitud penyerapan pada 1040 cm^{-1} yang berkaitan dengan peregangan simetri PO_2^- dalam DNA dan RNA berkurangan 10% atau lebih. Kesimpulannya, hasil kajian ini menunjukkan bahawa penggunaan nanopartikel Bi_2O_3 NPs sebagai pemeka sinaran tidak meningkatkan tindak balas RIBE secara signifikan pada sel yang tidak disasarkan.

EVALUATION OF RADIATION INDUCED BYSTANDER EFFECT (RIBE) INVOLVING MCF-7 AND HFOB 1.19 CELLS FOLLOWING BISMUTH OXIDES NANOPARTICLES TREATMENT IN RADIOTHERAPY

ABSTRACT

In radiotherapy, nanoparticles have been widely investigated as potential radiosensitizer to increase the radiation lethal effects on cancer cells. Targeted nanoparticles to the cancer cells might reduce the unnecessary radiation dose to healthy tissues. Nevertheless, the presence of nanoparticles might also trigger the responses of non-targeted cells to radiation or the radiation-induced bystander effect (RIBE). In this research, evaluation on the RIBE due to bismuth oxide nanoparticles (Bi_2O_3 NPs) application during radiotherapy in human breast cancer MCF-7 and normal osteoblast hFOB 1.19 cells were conducted. The studies were performed using external beam radiotherapy of photon and electron beams as well as high dose-rate (HDR) brachytherapy. RIBE stimulation was performed through a medium transfer technique. Reactive oxygen species (ROS), cell viability, cell survival, apoptosis assays and Fourier Transform Infrared (FTIR) spectroscopy were employed to evaluate the effect. The results demonstrated that MCF-7 and hFOB 1.19 bystander cells were able to maintain their proliferation for more than 80% after 48 hours incubation with irradiated-cell conditioned medium (ICCM) treated with Bi_2O_3 NPs. The bystander cells also present a positive response in their ability to sustain the survival up to 80% after treatment with ICCM for 10 days. The ROS level increased in the bystander cells, but the addition of Bi_2O_3 NPs did not significantly increase the ROS level. Observation on the apoptosis level in MCF-7 and hFOB 1.19

cells concerning the radiation dose or addition of Bi_2O_3 NPs compared to control group also present no significant increase. The absorbance levels at wavenumber 1080 cm^{-1} (symmetric PO_2^- stretching of the DNA) were almost identical for treated and untreated group of both cells. The amplitude of the peaks located at 1040 cm^{-1} corresponding to the symmetric PO_2^- stretching in DNA and RNA indicate changes approximately around 10%. In conclusion, the finding in this study provides evidence that the use of Bi_2O_3 NPs as radiosensitizer in radiotherapy does not significantly increase the RIBE responses in non-targeted cells.

CHAPTER 1

INTRODUCTION

1.1 Research Background

The incidence of cancer has been increasing over the years and it is the second leading cause of death globally (Teh & Woon, 2021). According to GLOBOCAN 2020, there was approximately 50,000 cancer cases have been reported in the year 2020 in Malaysia with breast cancer, lung cancer and colon cancer as the top three cases (World Health Organization, 2021). Radiation therapy or radiotherapy (RT) is one of the common and effective treatment for cancer disease (Feiock et al., 2016; Mi et al., 2016). The advantage of radiotherapy over other treatment choices owing to better survival, local control, and profiles of quality of life or toxicity (Rosenblatt et al., 2018). However, irradiation of cancer cells may also affect the nearby normal cells, thereby increasing the risk of second cancer in the future.

RT employs high energy ionizing radiation that directly kills the cancer cells and may also cause genetic changes resulting in cancer cell death (Baskar et al., 2012). The high energy radiation targeting the critical target of the cells which is deoxyribonucleic acid (DNA) of cells, leading to genetic material damage and blocking the cell's ability to divide and proliferate. Ionizing radiation may also indirectly damage the cells through a free radical generation that may harm the DNA of cells (Goel et al., 2017; Y. Liu et al., 2018). In an effort to improve the efficacy of cancer treatment, nanomaterials have been introduced to increase radiotoxicity to the

cancerous region and minimize the biological effect on normal cells (K. Song et al., 2013). Extensive investigations have been carried out by researchers regarding the enhancement of radiation toxicity on the targeted tumour cells through the application of radiosensitizer.

Metallic nanoparticle radiosensitizers such as gold nanoparticles (AuNPs), platinum nanoparticles (PtNPs) and iron oxide nanoparticles (Fe_3O_4 NPs) have been identified as radiosensitizers that can increase the effect of radiation on cancerous areas by increasing dose deposition in the target amount (Jackson et al., 2010; Khoshgard et al., 2017; Muhammad et al., 2018). Apart from that, previous research had proved that bismuth oxide nanoparticles (Bi_2O_3 NPs) also had the potential to act as a radiosensitizer in RT (Abdul et al., 2019; Abidin et al., 2019; Sisin et al., 2019). Bismuth oxide nanoparticles (Bi_2O_3 NPs) (Z = 83) is an alternative for a cost-effective and good candidate of high Z radiosensitizer. Furthermore, bismuth oxide and bismuth-based compounds are considered as one of the least toxic and biologically non-reactive heavy metals, biodegradable and biocompatible which is more suitable for *in-vivo* applications compared to other metals (Shahbazi et al., 2020; Stewart et al., 2016). Theoretically, bismuth has a higher Z number than gold. Therefore, it is predicted to demonstrate a promising potential as a dose-enhancing agent in radiation therapy (Alqathami et al., 2013).

The impact of nanoparticles on targeted cells has been studied extensively. However, the effect of nanoparticles on non-targeted cells during RT is poorly studied. The main concern is if the use of nanoparticles in RT causes a bystander effect or a non-targeted effect on adjacent healthy tissue. The response of the non-

irradiated cells to the radiation exposure is known as radiation-induced bystander effects (RIBE) (Marín et al., 2015). The bystander effect is an indirect radiation effect that affects untargeted cells that are not directly affected by radiation but suffer from nearby irradiated cells (Heuskin et al., 2013).

It is a concern that the employment of nanoparticles as radiosensitizers could be the factor that may boost the RIBE response and produce negative effects in non-irradiated adjacent cells (Rostami et al., 2016). The unclear results regarding RIBE mechanisms and the wide range of results from numerous experimental studies showed that the bystander effects or non-targeted effect research serve as an interesting area for debate in radiobiology studies (Desouky et al., 2015). RIBE responses are highly variable among the tested cells. They can be beneficial or hazardous depending on the cell lines, radiation dose, experimental end points and experiment time and duration (Verma & Tiku, 2017). It is considered harmful due to the cellular lesions that might be induced in the non-targeted cells due to bystander response from targeted cells (Temelie et al., 2016).

However, the non-targeted cells might be rescued from the effect of directly exposed cells through releasing of protective signals that were possibly induced by bystander responses (Pereira et al., 2014). In general, if the degree of damages induced by RIBE in tumour cells is superior to normal cells, it may help to enhance the therapeutic ratio (Soleymanifard & Toossi Bahreyni, 2012). The present study intended to examine the cellular status of bystander cells as a result of Bi_2O_3 NPs application during clinical beam irradiation. The RIBE responses between the normal

and cancerous cells after the incubation with irradiated-cell conditioned medium (ICCM) were investigated.

1.2 Problem Statement

The main challenge of radiation therapy is the unnecessary exposure to the adjacent normal tissue when high energy ionizing radiation is used to eradicate cancer cells (G. Song et al., 2017). The application of tumour-specific nanoparticles in radiation therapy can improve the radiotherapeutic outcomes by introducing more toxicity to the tumours and spare the normal tissues (Mesbahi, 2010). Radiosensitizers have been extensively studied in radiotherapy as an agent to enhance the effect of radiation in cancerous cells (Mi et al., 2016; Rostami et al., 2016). The presence of high Z atoms in the cancerous tissue intensifies the ionization process and enhances the dose deposition in the targeted area. The additional ionization generates series of Auger electron emissions which leads to further radiation interaction effects in the targeted area (Porcel et al., 2010).

The additional interaction of radiation with nanoparticles producing hydrolysis of water molecules within the cell, generating free radicals that can interact with DNA and subsequently cause huge numbers of DNA damage and cell death (Paro & Shanmugam, 2017). The main concern is the employment of nanoparticles as radiosensitizers could be the factor that may enhance the RIBE response and produce negative effects in non-irradiated adjacent cells (Rostami et al., 2016). Bystander cells or non-targeted cells could potentially experience the same

biological effect as targeted cells if the radiation effect is expanded due to the additional radiation interaction with radiosensitizer.

To date, numerous studies on RIBE employing *in-vitro* or *in-vivo* models have been conducted with several end points and using a distinct experiment protocol (Mitchell et al., 2004). However, the process underlying the bystander responses elicited by nanoparticles is uncertain and unknown. The implications of bystander signaling with the addition of nanoparticles as radiosensitizer are only beginning to be explored (P. Calatayud et al., 2015; Rostami et al., 2016). The effect of Bi_2O_3 NPs on RIBE has yet to be investigated. It is important to ensure that Bi_2O_3 NPs is safe to be used as radiosensitizer, especially to the adjacent healthy tissue. The effect of glucose-coated gold nanoparticles (Glu-GNP) on lung cancer and breast cancer bystander cells have been studied previously. The results showed that the bystander responses were produced in human lung cancer cells and no significant response coming from breast cancer cells (Rostami et al., 2016).

Breast cancer is one of leading cancer among women in the world (Terheyden et al., 2016). The irradiation of breast cancer may involve several types of tissue including part of the breastbone. In breast cancer patients, bone is the most prominent site of bone metastasis (Pulido et al., 2017). Bone metastasis is widespread in solid tumours with breast cancer contributing to 36% of the cases (Marazzi et al., 2020). Until now, the contribution of the bystander effect on the normal bone cells has not been widely investigated. Therefore, this study aims to evaluate the RIBE response in the normal bone osteoblast cells using Bi_2O_3 NPs application as radiosensitizer during clinical beam irradiation. A detailed study is

conducted to evaluate the induction of bystander effects between cancer and normal cells. The therapeutic ratio may be neutralized if the addition of nanoparticles to tumour cells results in bystander effects in normal cells.

More importantly, this analysis will assist the current efforts to specifically deliver nanoparticles to tumour cells while protecting the normal tissues. Without understanding the mechanism of RIBE produced by nanoparticles, it is impossible to determine their impact on the therapeutic ratio in radiotherapy. The results of this study will lay the foundation to understand bystander cell responses to radiation exposure with the application of Bi_2O_3 NPs.

1.3 Research Scope

In this *in-vitro* study, the RIBE stimulation was primarily focused on the medium transfer technique wherein the culture medium from the irradiated cells is the main mediator for triggering the bystander effect in the non-targeted cells. The culture medium treated with and without Bi_2O_3 NPs was collected and added into the non-irradiated cells to perceive whether the RIBE responses are increased or decreased with nanoparticles application. This study aimed to evaluate the RIBE response in between normal and cancer cells in several aspects including their ability to proliferate and survive and also the possible consequences such as ROS and apoptosis generation. The quantitative analysis was performed using Fourier Transform Infrared (FTIR) spectroscopy to observe the alteration or changes in the DNA of the treated cells as a result of Bi_2O_3 NPs application.

1.4 Objective of the Study

General Objective:

To investigate the effects of bismuth oxide nanoparticles (Bi_2O_3 NPs) on radiation-induced bystander effects (RIBE) in radiotherapy.

Specific objectives:

1. To evaluate the cytotoxicity and cellular internalization of bismuth oxide nanoparticles (Bi_2O_3 NPs) in the cells.
2. To measure and compare the bystander cell viability, survival rate and generation of reactive oxygen species (ROS) in the normal and cancer cells at different radiation doses.
3. To investigate RIBE response on cellular DNA structure quantitatively using Fourier Transform Infrared (FTIR) spectroscopy and the possibility of apoptosis induction in the bystander cells.
4. To assess the influence of different irradiation parameter radiation (type and energy) on RIBE.

1.5 Thesis Outline

This thesis has been divided into several chapters.

Chapter 1 (Introduction) - This chapter mainly discussed the research background, problem statements and also scope for this study. The research objectives were highlighted in this chapter.

Chapter 2 (Literature Review) – This chapter described the general idea about radiotherapy, radiobiology, and nanomedicine field. The challenges in these fields were also highlighted. The bystander effect induced by radiation during the application of nanoparticles was elucidated in this chapter.

Chapter 3 (Materials and Methods) – This chapter explained the detailed methodology involved in this study. This study conducted several analyses which are cytotoxicity assay, cellular uptake analysis, cell viability, cell survival analysis and reactive oxygen species (ROS) analysis. Apoptosis assay and Fourier Transform Infrared (FTIR) spectroscopy also have been conducted for details RIBE analysis.

Chapter 4 (Results and Discussion) – This chapter illustrated the findings and discussion for this study. It was divided into several sections, which are cytotoxicity and cellular uptake analysis, short term and long term effect of RIBE, generation of ROS, DNA damage in the bystander cells as well as apoptosis pathway in response to RIBE. The effect of different irradiation parameters on RIBE were also elucidated.

Chapter 5 (Conclusion) – This chapter summarized the findings for this study according to the research objectives.

CHAPTER 2

LITERATURE REVIEW

2.1 Radiotherapy and Challenges

The ultimate goals of radiotherapy are to maximize the lethal radiation dose to the cancer cells while minimize the exposure to normal cells. In contrast to cancer cells, the healing process for normal cells takes a shorter time and allows them to regain their normal functional state. However, cancer cells are not effective at restoring the damage caused by radiation therapy, results in differential cancer cells death (Baskar et al., 2012). There have been dramatic changes in the delivery of radiation therapy since 20 years ago. A major consideration to improve RT has been focused on dealing with the differences between the tumour and tissue characteristics which has been achieved by radiation-dose fractionation in the past (Schaue & Mcbride, 2015). The technology improvements are beneficial for clinical applications in RT, but increasing the radiation dose does not remarkably improve tumour control probability (TCP) for many radioresistant tumours (Y. Liu et al., 2018). In order to gain effective tumour control in radiation therapy, it is always restricted by the essential compromise in radiation toxicity to the normal tissue.

Nonetheless, the impact of RT on the radiobiological aspect is still an issue. The major drawback of RT is the lack of selection of cancer and healthy tissues due to similar mass energy absorption properties (Rosa et al., 2017). Another challenge in RT is that the location of tumours where its often located close to normal tissues and organs at risk (OARs). This situation limits the process to deliver radiation doses to

the target volumes (Y. Liu et al., 2018). The introduction of high-atomic number (Z) material into the targeted cells is an approach to enhance the differential response between tumour and normal tissue response (Haume et al., 2016; Rosa et al., 2017). High Z materials specifically metals such as gold nanoparticles (AuNPs), generally display chemical inertness which helps to decrease potential hazards in cellular systems in living tissue (Y. Liu et al., 2018). Metal-based nanoparticles with high Z have also been found as an effective radiotoxicity agent to improve the contrast between tumour and soft tissues. Metal-based nanoparticles with high Z offer radiosensitization properties to improve the tumour control, surges healthy cell survival and minimize the side effects when using RT alone (Rosa et al., 2017).

2.2 Radiation Biology

2.2.1 Radiobiology and Radiation Injury Mechanism

Radiobiology is a field of study that involves a combination of basic principles of physics and biology which concern with the action or effect of ionizing radiation on single cells or parts of cells in the living tissue (Podgorsak, 2006). Living organisms are continuously exposed to ionizing radiations from natural radiation or artificial radiation which causes injury to cells through the ionization of atoms or molecules (IAEA, 2010). High-energy radiation damages genetic material or DNA of cells and interrupts cell's ability to divide and proliferate further (Baskar et al., 2014).

Irradiation of any biological or living tissue triggered a response that varies in the time scale. As shown in Figure 2.1, radiation reactions can be classified into three

types: physical, chemical, and biological. The physical phase is the interaction between the radiation beam or particles with the atom of the tissue. It takes about 10^{-18} seconds for high-speed radiation energy to traverse the DNA molecules. It interacts with the orbital electron or nuclei, ejecting some of them or raising them to a higher energy level. This situation results in ionization or excitation of the atom in biological tissue (van der Kogel, 2009).

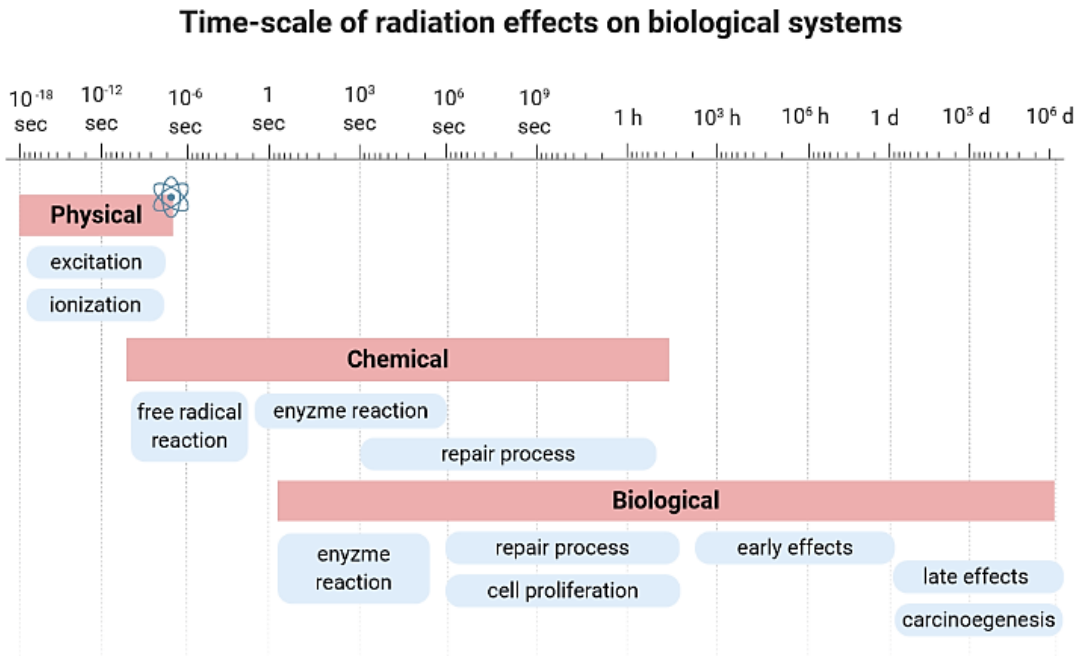

Figure 2.1 The time-scale of radiation effects on biological systems (adapted from van der Kogel, 2009).

The chemical phase is defined as the period in which the chemical reaction occurs between the damaged atoms and molecules with other cellular components. The breakage of chemical bonds and formation of free radicals arise due to the ionization and excitation process. Free radical reaction may occur within approximately 1 millisecond of irradiation. In the chemical phase, several processes happened including the scavenging reactions for inactivating the free radical and also

the fixation reaction to stabilize the chemical changes in molecules (van der Kogel, 2009).

All subsequent biological responses of the ionizing radiation interaction are related to the biological phase. As a consequence of direct ionizing radiation interaction with cell structures or indirect effect through water radiolysis process, biological effects attributed to irreparable or misrepaired DNA damage in cells may arise. The possible biological effects related to radiation interaction with living tissue are cell death, chromosomal aberrations, DNA damage, cell cycle arrest, apoptosis, mutagenesis, and carcinogenesis (Desouky et al., 2015; Zhao et al., 2019). The observable effects of ionizing radiation may occur up to several years after exposure (van der Kogel, 2009).

Radiation injury to the cell can be caused by two possible ways; (1) the direct action of radiation on the DNA molecules or (2) the indirect action of radiation on the DNA molecules through the water molecules. The major effect of ionizing radiation on tissues is the depopulation of cell populations and followed by tissue functional deficiency due to direct cell killing mostly by damaging the DNA (Baskar et al., 2014). The direct and indirect radiation injury mechanism on DNA molecules was illustrated in Figure 2.2.

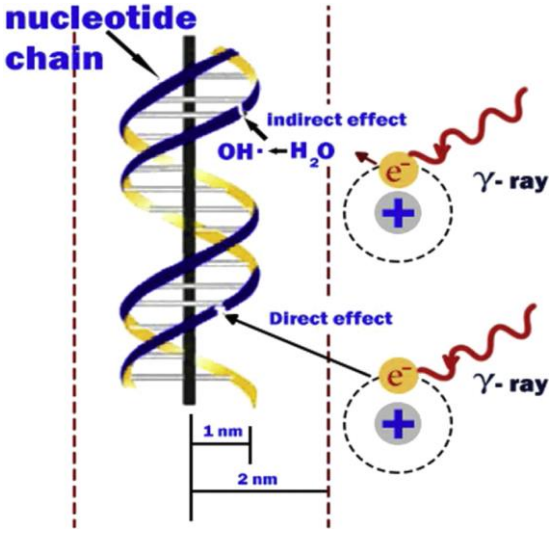

Figure 2.2 The possible radiation injury mechanism, direct and indirect actions of radiation (adapted from Desouky et al., 2015).

In the direct action of radiation, the cellular molecules and DNA of the cells is directly hit by radiation result in disrupting the molecular structure. As depicted in Figure 2.3, radiation may directly create single-strand break (SSBs) and double-strand breaks (DSBs) to the DNA molecules. The structural change of the DNA causes cell damage or cell death. The damaged cells that survived may induce carcinogenesis, abnormalities and mutagenesis (Desouky et al., 2015). Cellular response to ionizing radiation depends on linear energy transfer (LET) of radiation, type and energy of radiation, radiation dose and cell type as well as cell sensitivity (Prise et al., 2005). The high-LET radiations such as α-particles and neutrons and high radiation doses mainly interact through direct action (Desouky et al., 2015).

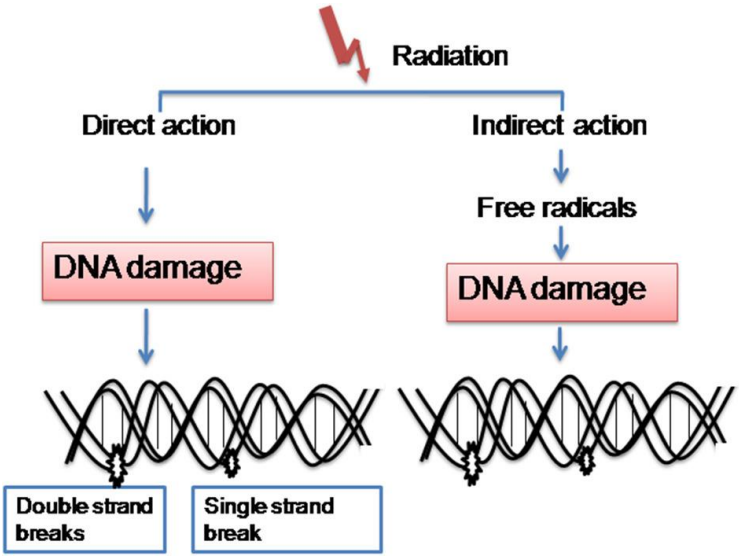

Figure 2.3 Two ways of radiation action (adapted from Baskar et al., 2014).

In the indirect action, the water molecules which is the major component of the cell is the main target for radiation interaction. This indirect interaction is called water radiolysis (IAEA, 2010). Free radicals are the subsequent result from the ionization or excitation of water components in the cells (Baskar et al., 2014). This process produces the free radicals' products such as hydroxyl (HO•) and alkoxy (RO2•). The free radicals can diffuse in a long distance to reach and harm critical targets (Desouky et al., 2015; Hall, 2010).

A free radical refers to an atom or molecule with unpaired electrons or odd number of electron in the valence shell or outer shell (Hall & Giaccia, 2006). A free radical is unstable, short-lived and extremely reactive. They can interact with electrons from other compounds to attain stability due to their high reactivity. The attacked molecule becomes a free radical when loses its electron, followed by a chain reaction cascade which may damage the living cells (Phaniendra et al., 2015). The result of indirect action of radiation on DNA molecules is the losing cell function or death of the cell. The primary free radicals have an extremely short

lifetime, roughly 1^{-10} seconds (Hall & Giaccia, 2006). Around 60% of cellular damage in low LET ionizing radiations such as X-rays and gamma-rays are caused by indirect action mechanism because of composition water nearly 70% in the cells (Baskar et al., 2014; Desouky et al., 2015).

The transfer or absorption of ionizing radiation energy to the biological material results in chemical bonds breakage and causes ionization of atoms and molecules such as water and other essential macromolecules including DNA, membrane lipids and proteins (Somosy, 2000). The biological effects of radiation primarily result from damage to the most critical target within the cell which is DNA. DNA is a large molecule with a double-helix structure, consist of two strands held by hydrogen bonds between the bases. The DNA strand backbone is made of sugar and phosphate groups (Wood, 2016).

A wide range of lesions in DNA may occur when cells are irradiated with X-rays such as SSBs, DSBs, protein-DNA, crosslinks base damage, and protein-protein crosslinks (Hall, 2010; Sofińska et al., 2020). The SSBs of DNA involve many breaks of a single strand in the phosphodiester linkage. In SSBs, cells are able to repair, but mutation can occur when the repair is incorrect or mismatch. The DSBs of DNA occur when there is a breakage in the two strands opposite to one another or separated by few base pairs. The tendency of DSBs to occur is about 0.04 times that of SSBs and they are induced linearly with dose (Hall & Giaccia, 2006; IAEA, 2010). It is expected that 1 Gy of radiation exposure will result in 20 to 40 DSBs per cell. The unrepaired DSBs may lead to cellular lethality (Golden et al., 2012).

Several consequences may occur upon irradiation of cells including division or mitotic delay, apoptosis, reproductive failure, genomic instability, mutation, cell transformation, bystander effect and adaptive responses. The irradiated cell might encounter a delay in their normal cell division. Apoptosis may happen if the cell dies before it can divide or fragmented into smaller bodies and be absorbed by neighbouring cells. Reproductive failure occurs when the cells die during the first or subsequent mitosis. The irradiated cell may also have genomic instability which may result in reproductive failure. The cells can survive from irradiation, but sometimes they may contain a mutation that can affect the offspring. The survived cell possibly experiences mutation result in a transformation of their phenotype and cause carcinogenesis. In addition, the bystander effects induced by radiation may appear when an irradiated cell transmits signals to neighboring or adjacent cells. The adaptive responses can occur when the irradiated cells become more resistant to following irradiation (Podgorsak, 2005).

Cell death or “killed” by radiation refers to the loss of a specific function, loss of reproductive integrity or reproductive death due to unsuccessful cell divisions after irradiation (Podgorsak, 2006). Cell death mechanisms are through apoptosis, necrosis, autophagy, mitotic catastrophe and cell senescence and radiation-induced differentiation DNA (Hall & Giaccia, 2006; van der Kogel, 2009). The illustration of different radiation-induced cell death mechanisms is presented in Figure 2.4. The cell death mechanism depends on numerous factors including the radiation dose and quality, cell type, oxygen tension, p53 mutation status, DNA repair capacity, redox state, and cell cycle phase during radiation exposure (Golden et al., 2012).

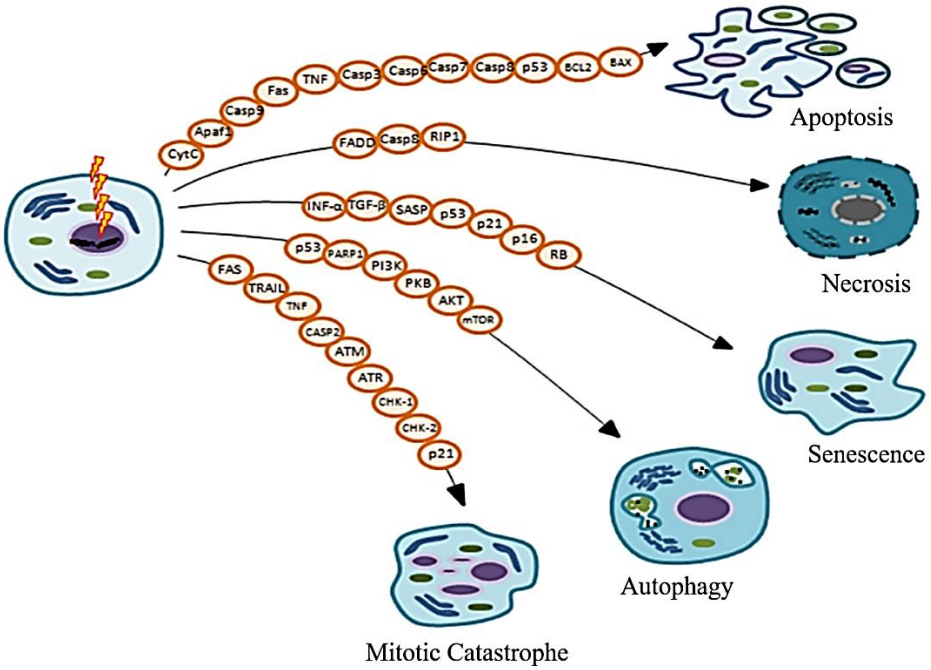

Figure 2.4 The illustration of different radiation-induced cell death mechanisms (adapted from Minafra & Bravatà, 2015).

Most of the damage induced in the cells by radiation may be repaired by multiple enzymatic mechanisms of DNA. Repair refers to the process by which the function of macromolecules is restored. DNA strand breaks may be rejoined but it does not necessarily mean that gene function is restored. Rejoining can leave a genetic defect or mutation in the cells (van der Kogel, 2009). Recovery of the cellular or tissue refers to the increase in cell survival or reduction in the extent of radiation damage to tissue if there is sufficient time is allowed for this recovery to take place. The repair mechanisms for each DNA lesion in cells are different and depend on the type of lesion. The mechanisms used to repair base damage are different from the mechanism used to repair strand breaks. Different repair pathways are used to repair DNA damage and its related to the stage of the cell cycle (Hall & Giaccia, 2006). For instance, DSBs induced by radiation in an S phase cell would benefit from the cell preventing DNA replication until the break is repaired.

There are several enzymatic mechanisms involved in DNA repair in cells that act on different types of lesions. For DSBs, there are two primary repair pathways, non-homologous end joining (NHEJ) and homologous recombination (HR). NHEJ repair works on blunt-ended DNA fragments resulting from broken phosphodiester linkages. Repair by NHEJ operates throughout the cell cycle but it dominates in G_1/S-phases. The process is likely to error because it does not rely on sequence homology. DSB repair by HR employs sequence homology with an undamaged copy of the broken region and hence can only operate in late S or G_2 phases of the cell cycle. Other DNA repair mechanisms such as base excision repair (BER), mismatch repair (MR) and nucleotide excision repair (NER) respond to damage such as base oxidation, alkylation, and strand intercalation (IAEA, 2010).

2.2.2 Non-Targeted Effect of Radiation

Traditionally, it was believed that effects of ionizing radiation are due to direct ionization of cell structures particularly DNA, or from indirect damage through reactive oxygen species produced by water radiolysis (Desouky et al., 2015). The biological effects of ionizing radiation are assumed to be limited to cells and tissues within the target or treatment area. However, this traditional belief has been challenged by the existence of radiation-induced bystander effects (RIBE) or non-targeted effects (Marín et al., 2015). In other words, the ionizing radiation effect may also affect the non-irradiated neighbouring cells or tissues. As illustrated in Figure 2.5, the consequences of radiation interaction on irradiated cells towards unirradiated cells or also known as the bystander effect have been studied hundred years ago. The

bystander effect involves the radiation response induced in the unirradiated cells located near the irradiated cells.

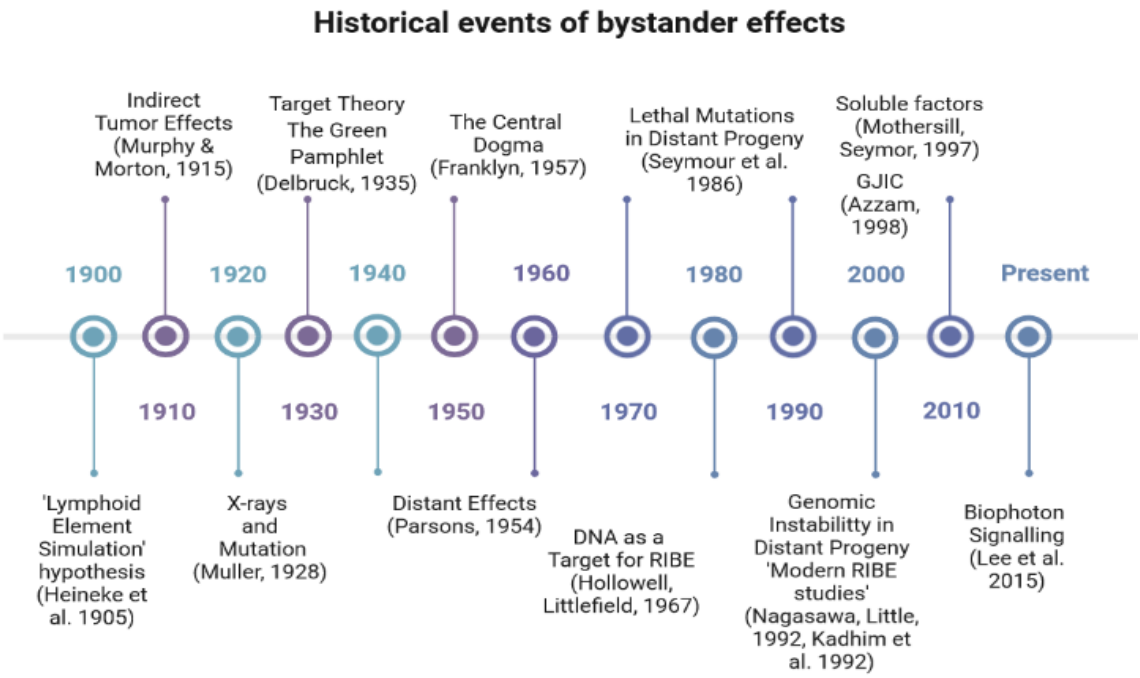

Figure 2.5 A timeline on bystander effects study over the last hundred years. (adapted from Carmel Mothersill, Rusin, Fernandez-Palomo, & Seymour, 2017).

In addition to bystander effects, two other classifications of signaling-mediated radiation effects are abscopal and cohort effects (R. Wang et al., 2018). The classifications of radiation-induced signaling are shown in Figure 2.6. The radiation triggered a response in the cells located further away from the radiation field is known as the abscopal effect (Desouky et al., 2015; Pouget et al., 2018). The abscopal effect is the phenomenon whereby irradiated tissues may possibly transmit the signals to the unirradiated tissues located outside the irradiated volume (Carmel Mothersill et al., 2017; R. Wang et al., 2018). The abscopal effect is related to the clinical changes observed due to the radiation effect, while the bystander effect refers to radiobiological events in unirradiated cells coming from the radiation effect

(Desouky et al., 2015). In general, abscopal effects can be observed in patients with metastatic cancers receiving radiotherapy. In other words, the irradiation to a specific part of the body produced chromosomal damage and cellular alterations in distant tissues (R. Wang et al., 2018).

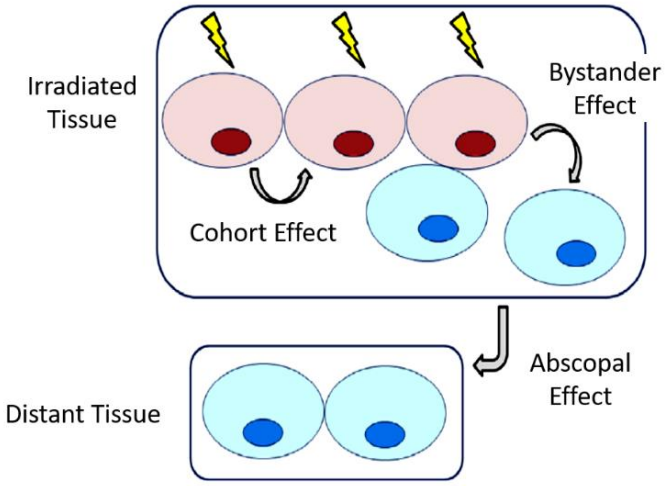

Figure 2.6 Schematic representation of radiation-induced signaling effects in non-targeted and targeted cells. Irradiated cells are shown in red; unirradiated cells in blue (adapted from Butterworth et al., 2013).

Another non-targeted effect identified in radiation therapy is the cohort effect. The cohort effect demonstrates a phenomenon where irradiated cells release signals that decrease the neighbouring cells survival within an irradiated field or volume. This situation describes the overall radiobiological responses is not owing to the consequence of direct energy deposition in the target cell, but might be associated with the cellular communication within an irradiated volume (Blyth & Sykes, 2011; Butterworth et al., 2013; R. Wang et al., 2018).

2.3 Radiation-Induced Bystander Effect

Generally, the biological effects of ionizing radiation are mostly attributed to specific targeting to the nucleus that results in DNA damage (Marín et al., 2015). However, experiments in the previous decade have demonstrated the existence of a 'bystander effect'. Based on the report by Nagasawa and Little in 1992 following low dose irradiation from α-particles, a larger proportion of cells exhibited biological damage compared to the proportion of cells hit by an α-particle. Initially, only 1% of the cells undergone nuclear traversal, but 30% increase in sister chromatid changes has been observed (Hall & Giaccia, 2006). S. G Sawant and co-workers observed the same effect in which exposure of 10% of the cells to alpha particles, resulting in a greater frequency of oncogenic transformation in the cell population (Sawant et al., 2001).

A situation where cells that have not been directly exposed to ionizing radiation behave in the same way as the irradiated or exposed cells is known as radiation-induced bystander effect (RIBE) (Carmel Mothersill & Seymour, 2004). In the other words, the non-irradiated cells may respond to the radiation exposure on the targeted cells. Exposure to ionizing radiation may affect the cells directly targeted and also indirectly affect the non-irradiated adjacent neighbours. Based on the timescale, the direct effect and indirect effect of ionizing radiation may show up approximately 1×10^{-6} seconds after irradiation (Österreicher et al., 2003). But bystander effect turned up at a slower rate because they started to activate after the chemical factors release in the first few hours post-irradiation and the endpoint in the

period from 3 hours to 60 hours post-irradiation (Carmel Mothersill & Seymour, 1997).

The signal received from irradiated cells resulted in several biological phenomena in neighboring and distant unirradiated cells involve harmful effects such as chromosomal aberrations, cell killing, mutation, oncogenic transformation, gene expression alteration and inflammatory mediator production as well as beneficial effects such as shrinkage of metastases phenomena (Hall & Giaccia, 2006; Marín et al., 2015; Carmel Mothersill & Seymour, 2004). In addition, the cells that experience bystander effects imitate the other effects experienced by irradiated cells such as DNA damage, micronucleation, apoptosis, proteins and enzymes regulatory alteration and clonogenic inefficiency (Marín et al., 2015). The RIBE has the potential for killing tumour cells and cause damage to the normal tissue (Toossi et al., 2014). The existence of bystander phenomena indicates that the nucleus of the cells is not the only target for radiation, but also the surrounding of the cell itself.

Over the years, the attention in radiobiological studies has been extended to the non-targeted effects of adjacent tissue surrounded the targeted area or field of radiation. Since the first observation of RIBE in 1992, numerous studies have been carried out to investigate this phenomenon. The bystander effect involved the biological response in cells that are not directly hit by ionizing radiation but the response to the signals producing in the targeted cells (Mitchell et al., 2004). The bystander cells might be adjacent or distant away from the exposed cells (Rostami et al., 2016). In other words, any cells that surround the irradiated cells can be a bystander cells. The classification of bystander cells can be adjacent cells, a cell

within few diameters from targeted cells, cells in a different organ or even in a different animal to the irradiated cells (Blyth & Sykes, 2011).

The bystander effect has been studied through medium transfer from irradiated cells and co-culturing the cells to induce cell-to-cell interaction. An earlier study on bystander effects was typically carried out using microbeam to estimate the non-targeted effect on the surrounding cells. Apart from co-culturing, there is also a report on biologic effects due to bystander effects using another method of experiment, in which the culture medium from irradiated cells was transferred to the unirradiated cells. When irradiation media is transferred into unirradiated cells, the irradiated cells release chemicals into the medium and have the ability to affect the unirradiated cells. (Hall & Giaccia, 2006; van der Kogel, 2009). Irradiation might lead to an increase in levels of long-lived reactive oxygen species (ROS) that could trigger a response in both irradiated and unirradiated cells. A brief outline of RIBE is shown in Figure 2.7.

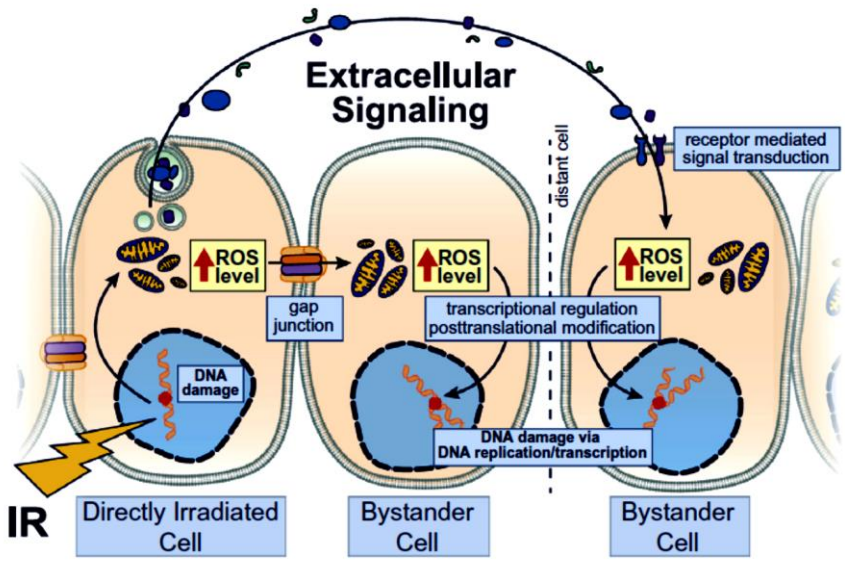

Figure 2.7 A model of radiation-induced bystander effect (RIBE) responses in the cells (adapted from Klammer, Mladenov, Li, & Iliakis, 2015).

2.4 Cell Signaling, Communication and Bystander Effect Pathways

Cellular components in living tissue can respond and react to the changes in the adjacent environment due to cell's ability to receive, absorb and process the signals that originate from outside of their boundaries. Individual cells can receive many signals instantaneously. The cells also transmit the messages and signals to the other near or distant cells (Alberts et al., 2002). There are mechanisms that enable one cell to influence the behavior of other cells. Signal molecules bind to cell-surface receptors can generate more signals inside the target cell as illustrated in Figure 2.8.

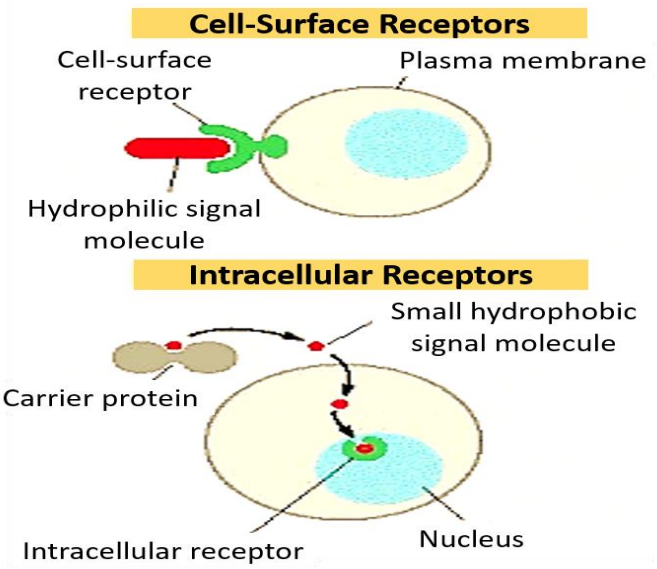

Figure 2.8 The binding of extracellular signal molecules to either cell-surface receptors or intracellular receptors (adapted from Alberts et al., 2002).

The studies have proven that the targeted cells release molecular signals or factors which may produce genetic alteration, reduce cell proliferation, introduce cell death and DNA damage, arrest the cycle of the cells and also release some protein expression in non-irradiated cells following irradiation (Desai et al., 2013; Soleymanifard et al., 2013, 2016; Temelie et al., 2016; Tu et al., 2019). The nature